

Electron recombination with multicharged ions via chaotic many-electron states

V. V. Flambaum¹, A. A. Gribakina[†], G. F. Gribakin², and C. Harabati¹

¹*School of Physics, The University of New South Wales, Sydney, UNSW 2052, Australia*

²*Department of Applied Mathematics and Theoretical Physics, Queen's University, Belfast BT7 1NN, UK*

(October 27, 2018)

Abstract

We show that a dense spectrum of chaotic multiply-excited eigenstates can play a major role in collision processes involving many-electron multicharged ions. A statistical theory based on chaotic properties of the eigenstates enables one to obtain relevant energy-averaged cross sections in terms of sums over single-electron orbitals. Our calculation of the low-energy electron recombination of Au^{25+} shows that the resonant process is 200 times more intense than direct radiative recombination, which explains the recent experimental results of Hoffknecht *et al.* [J. Phys. B **31**, 2415 (1998)].

In this paper we give a quantitative explanation of the puzzle of electron recombination with Au^{25+} . We also demonstrate how to calculate the contribution of “chaotic” multiply-excited states of the compound ion, which mediate electron recombination with complex many-electron ions.

Experimentally, this process was studied recently at the UNILAC heavy ion accelerator facility of the GSI in Darmstadt [1]. In spite of a high energy resolution [2] the measured recombination rate did not reveal any resonances and only showed two broad structures around 30 and 80 eV. However, its magnitude at low electron energies $\varepsilon \sim 1$ eV exceeded the radiative recombination (RR) rate by a factor of 150 [3], although the observed energy dependence was close to that of RR.

It is well-known that recombination rate can be enhanced by dielectronic recombination (DR). In this process the incident electron is captured in a doubly-excited state of the compound ion, which is then stabilised by photoemission. Suggested originally by J. Sayers, it was first considered by Massey and Bates [4] in the problem of ionospheric oxygen. Later DR was found to be important for the ionization balance in the solar corona and high-temperature plasmas on the whole [5]. Electron-ion recombination has been measured directly in the laboratory since early 1980’s [6]. More recently the use of heavy-ion accelerators and electron coolers of ion storage rings has greatly advanced the experiment [7,8]. Recombination rates for many ions have been measured from threshold to hundreds of eV electron energies with a fraction-of-eV resolution [9–15]. For few-electron ions the measured rates were in good agreement with theory which added the contribution of DR resonances to the RR background, e.g., He^+ [16], Li-like C^{4+} [15] and Ar^{15+} [9,14], and B-like Ar^{13+} [17]. However, more complicated ions, e.g., Au^{51+} [13] and U^{28+} [12], showed complicated resonance spectra and strongly-enhanced recombination rates at low electron energies. In particular, in U^{28+} the theory was able to explain the main resonant features in the range 80–180 eV, but failed to identify the resonances and reproduce the rate at smaller energies [18]. The situation in Au^{25+} [1] looks even more puzzling.

In Ref. [19] we suggested that electron recombination with Au^{25+} is mediated by complex *multiply-excited* states of Au^{24+} , rather than “simple” dielectronic resonances. Electrons could be captured in these states due to a strong configuration interaction in this open-shell system (the ground state of Au^{24+} is $4f^9$). The single-particle spectrum of Au^{24+} does not have large gaps, see Fig. 1. Using the single-particle orbitals we generated many-electron configurations, evaluated their energies and estimated the energy density of multiply-excited states [19]. Owing to the “gapless” single-particle spectrum, the density increases rapidly as a function of energy, as described by the Fermi-gas-model ansatz [20]

$$\rho(E) = AE^{-\nu} \exp(a\sqrt{E}), \quad (1)$$

with $A = 31.6$, $\nu = 1.56$, $a = 3.35$ a.u. [21], where E is the energy above the ground state in atomic units used throughout the paper.

The excited states are characterised by their total angular momentum and parity J^π , and are $2J + 1$ times degenerate. Therefore the total level density is a sum of partial level densities: $\rho(E) = \sum_{J^\pi} (2J + 1) \rho_{J^\pi}(E)$. The spectrum of Au^{24+} near the ionization threshold, $E = I \approx 27.5$ a.u., contains J from $\frac{1}{2}$ to $\frac{35}{2}$ [19]. Their distribution is in agreement with statistical theory, $\rho_{J^\pi} \propto f(J)$, where

$$f(J) = \frac{2(2J+1)}{(2J_m+1)^2} \exp \left[-\frac{(2J+1)^2}{2(2J_m+1)^2} \right], \quad (2)$$

J_m being the most abundant value of J [20,22]. Numerically we find $J_m \approx \frac{9}{2}$. Using Eq. (2) we can estimate the partial densities by $\rho_{J^\pi} = f(J)\rho/\langle 2J+1 \rangle$, where $\langle 2J+1 \rangle$ is an average over $f(J)$. For the most abundant J values this leads to $\rho_{J^\pi}(E) = A_{J^\pi} E^{-\nu} \exp(a\sqrt{E})$ with $A_{J^\pi} \approx 0.15$. Near the ionization threshold we have $\rho_{J^\pi} \approx 3.6 \times 10^4$ au, which means that the spacing between the multiply-excited states with a given J^π is very small: $D = 1/\rho_{J^\pi} \sim 1$ meV. This would explain why autoionising resonances could not be observed in electron recombination with Au²⁵⁺ [19]. However, the large density is only a “kinematic” reason behind the experimental finding, because we have not proved that the electron can actually be captured in the multiply excited states. In what follows we analyse the dynamics of electron capture and show that the Coulomb interaction between the electrons makes the capture efficient and accounts for the observed enhanced recombination rate.

Taking into account this interaction is the key problem in many-electron processes. In general, this can be achieved by constructing a basis of many-electron states Φ_k from single-particle orbitals, and solving the eigenproblem for the Hamiltonian matrix $H_{ik} = \langle \Phi_i | \hat{H} | \Phi_k \rangle$, which yields the eigenvalues E_ν and eigenstates $|\Psi_\nu\rangle = \sum_k C_k^{(\nu)} |\Phi_k\rangle$ of the system (configuration interaction method). For open-shell systems with a few valence electrons, e.g., rare-earth atoms, this becomes an increasingly difficult task. The density of states grows very rapidly with the excitation energy, and finding the eigenstates requires diagonalisation of ever greater matrices.

On the other hand, when the level density is high and the two-body interaction is sufficiently strong the system is driven into a regime of *many-body quantum chaos*, where the effect of configuration mixing can be described statistically. In this case each eigenstate contains a large number N of *principal* components $C_k^{(\nu)} \sim 1/\sqrt{N}$, corresponding to the basis states Φ_k which are strongly mixed together. This strong mixing takes place in a certain energy range $|E_k - E_\nu| \lesssim \Gamma_{\text{spr}}$, where $E_k \equiv H_{kk}$ is the mean energy of the basis state and Γ_{spr} is the so-called *spreading width*. More precisely, the mean-squared value of $C_k^{(\nu)}$ as a function of $E_k - E_\nu$, is described by a Breit-Wigner formula

$$\overline{|C_k^{(\nu)}|^2} = N^{-1} \frac{\Gamma_{\text{spr}}^2/4}{(E_k - E_\nu)^2 + \Gamma_{\text{spr}}^2/4}, \quad (3)$$

with $N = \pi\Gamma_{\text{spr}}/2D$ fixed by normalisation $\sum_k |C_k^{(\nu)}|^2 \simeq \int \overline{|C_k^{(\nu)}|^2} dE_k/D = 1$. The decrease of $C_k^{(\nu)}$ for $|E_k - E_\nu| > \Gamma_{\text{spr}}$ is a manifestation of perturbation theory: the admixture of distant basis states is suppressed by large energy denominators. Apart from this systematic variation the components $C_k^{(\nu)}$ behave as Gaussian random variables.

This picture of many-body quantum chaos is supported by numerical studies of nuclei [24], complex atoms [25] and ions [19]. In particular, Ref. [19] provides an estimate of the spreading width in Au²⁴⁺: $\Gamma_{\text{spr}} \approx 0.5$ a.u. Hence, a typical eigenstate near the ionization threshold contains $N \sim 2 \times 10^4$ principal components.

For low-energy electrons the contribution of multiply-excited autoionising states (resonances) to the recombination cross section is [26]

$$\sigma_r = \frac{\pi}{k^2} \sum_{\nu} \frac{2J+1}{2(2J_i+1)} \frac{\Gamma_{\nu}^{(r)}\Gamma_{\nu}^{(a)}}{(\varepsilon - \varepsilon_{\nu})^2 + \Gamma_{\nu}^2/4}, \quad (4)$$

where $\varepsilon = k^2/2$ is the electron energy, J_i is the angular momentum of the initial (ground) target state, J are the angular momenta of the resonances, $\varepsilon_{\nu} = E_{\nu} - I$ is the position of the ν th resonance relative to the ionization threshold of the compound (final-state) ion, and $\Gamma_{\nu}^{(a)}$, $\Gamma_{\nu}^{(r)}$, and $\Gamma_{\nu} = \Gamma_{\nu}^{(r)} + \Gamma_{\nu}^{(a)}$ are its autoionisation, radiative, and total widths, respectively [27]. When the resonance spectrum is dense, σ_r can be averaged over an energy interval $\Delta\varepsilon$, $D \ll \Delta\varepsilon \ll \varepsilon$, yielding

$$\bar{\sigma}_r = \frac{2\pi^2}{k^2} \sum_{J\pi} \frac{2J+1}{2(2J_i+1)D} \left\langle \frac{\Gamma_{\nu}^{(r)}\Gamma_{\nu}^{(a)}}{\Gamma_{\nu}^{(r)} + \Gamma_{\nu}^{(a)}} \right\rangle, \quad (5)$$

where $\langle \dots \rangle$ means averaging. The fluorescence yield $\omega_f \equiv \Gamma_{\nu}^{(r)}/(\Gamma_{\nu}^{(r)} + \Gamma_{\nu}^{(a)})$, fluctuates weakly from resonance to resonance (see below), which allows one to write $\bar{\sigma}_r = \bar{\sigma}_c \omega_f$, where

$$\bar{\sigma}_c = \frac{\pi^2}{k^2} \sum_{J\pi} \frac{(2J+1)\Gamma^{(a)}}{(2J_i+1)D} \quad (6)$$

is the energy-averaged capture cross section, and $\Gamma^{(a)}$ is the average autoionisation width.

Unlike complex multiply-excited states Ψ_{ν} , the initial state of the recombination process is simple. It describes an electron with the energy ε incident on the ground state Φ_i of the target (e.g., $\text{Au}^{25+} 4f^8$, $J_i = 6$). The autoionisation width is then given by perturbation theory as

$$\begin{aligned} \Gamma_{\nu}^{(a)} &= 2\pi |\langle \Psi_{\nu} | \hat{V} | \Phi_i; \varepsilon \rangle|^2 \\ &= 2\pi \sum_{k,k'} C_k^{(\nu)*} C_{k'}^{(\nu)} \langle \Phi_i; \varepsilon | \hat{V} | \Phi_{k'} \rangle \langle \Phi_k | \hat{V} | \Phi_i; \varepsilon \rangle, \end{aligned} \quad (7)$$

where \hat{V} is the electron Coulomb interaction, and the continuum states ε are normalised to unit energy interval. Averaging $\Gamma_{\nu}^{(a)}$ over the chaotic states ν with $E_{\nu} \approx I + \varepsilon$, we make use of the fact that their components are random and uncorrelated, which leads to

$$\Gamma^{(a)} = 2\pi \sum_k \overline{|C_k^{(\nu)}|^2} |\langle \Phi_k | \hat{V} | \Phi_i; \varepsilon \rangle|^2. \quad (8)$$

Being a two-body operator, \hat{V} can move only two electrons at a time. A nonzero contribution to $\Gamma^{(a)}$ is given by the basis states which differ from the initial state $|\Phi_i; \varepsilon\rangle$ by the positions of two electrons. Therefore, in Eq. (8) we only need to sum only over *doubly-excited* basis states Φ_d . With the help of Eq. (3) the capture cross section (6) becomes

$$\bar{\sigma}_c = \frac{\pi}{k^2} \sum_d \frac{2J+1}{2(2J_i+1)} \frac{\Gamma_{\text{spr}} 2\pi |\langle \Phi_d | \hat{V} | \Phi_i; \varepsilon \rangle|^2}{(E_d - I - \varepsilon)^2 + \Gamma_{\text{spr}}^2/4}. \quad (9)$$

This form makes it clear [cf. Eq. (4)] that the two-electron excitations Φ_d play the role of *doorway states* for the electron capture process. Since these states are not the eigenstates of the system they have a finite energy width Γ_{spr} .

The wave function of a doorway state can be constructed using the creation-annihilation operators, $|\Phi_d\rangle = a_\alpha^\dagger a_\beta^\dagger a_\gamma |\Phi_i\rangle$, where $\alpha \equiv n_\alpha l_\alpha j_\alpha m_\alpha$ and $\beta \equiv n_\beta l_\beta j_\beta m_\beta$ are excited single-electron states, and $\gamma \equiv n_\gamma l_\gamma j_\gamma m_\gamma$ corresponds to a hole in the target ground state. (Note that we are using relativistic Dirac-Fock orbitals $nljm$.) Of course, to form doorway states with a given J the angular momenta of the electrons and ionic residue must be coupled into the total angular momentum J . However, the $2J + 1$ factor and summation over J implied in Eq. (9) account for all possible couplings, and we can simply sum over the single-electron excited states α , β and hole states γ , as well as the partial waves lj of the continuous-spectrum electron ε . As a result, we have

$$\bar{\sigma}_c = \frac{\pi^2}{k^2} \sum_{\alpha\beta\gamma, lj} \frac{\Gamma_{\text{spr}}}{(\varepsilon - \varepsilon_\alpha - \varepsilon_\beta + \varepsilon_\gamma)^2 + \Gamma_{\text{spr}}^2/4} \sum_\lambda \frac{\langle \alpha, \beta \| V_\lambda \| \gamma, \varepsilon lj \rangle}{2\lambda + 1} \times \left[\langle \alpha, \beta \| V_\lambda \| \gamma, \varepsilon lj \rangle - (2\lambda + 1) \sum_{\lambda'} (-1)^{\lambda+\lambda'+1} \left\{ \begin{matrix} \lambda & j_\alpha & j \\ \lambda' & j_\beta & j_\gamma \end{matrix} \right\} \langle \alpha, \beta \| V_{\lambda'} \| \varepsilon lj, \gamma \rangle \right], \quad (10)$$

where ε_α , ε_β and ε_γ are the orbital energies, and $\langle \alpha, \beta \| V_\lambda \| \gamma, \varepsilon lj \rangle$ is the reduced Coulomb matrix element [28]. The above equation is directly applicable to targets with closed-shell ground states. If the target ground state contains partially occupied orbitals, a factor

$$\frac{n_\gamma}{2j_\gamma + 1} \left(1 - \frac{n_\alpha}{2j_\alpha + 1} \right) \left(1 - \frac{n_\beta}{2j_\beta + 1} \right), \quad (11)$$

where n_α , n_β , and n_γ are the orbital occupation numbers in the ground state Φ_i , must be introduced on the right-hand side of Eq. (10). Steps similar to those that lead to Eq. (10) were used to obtain mean-squared matrix elements of operators between chaotic many-body states [25,29].

Chaotic nature of the multiply-excited states Ψ_ν can also be employed to estimate their radiative widths $\Gamma_\nu^{(r)}$. Electron-photon interaction is described by a single-particle dipole operator \hat{d} . Any excited electron in Ψ_ν may emit a photon, thus leading to radiative stabilisation of this state. The total photoemission rate $\Gamma_\nu^{(r)}$ can be estimated as a weighted sum of single-particle rates,

$$\Gamma_\nu^{(r)} \simeq \sum_{\alpha, \beta} \frac{4\omega_{\beta\alpha}^3}{3c^3} |\langle \alpha \| \hat{d} \| \beta \rangle|^2 \left\langle \frac{n_\beta}{2j_\beta + 1} \left(1 - \frac{n_\alpha}{2j_\alpha + 1} \right) \right\rangle_\nu, \quad (12)$$

where $\omega_{\beta\alpha} = \varepsilon_\beta - \varepsilon_\alpha > 0$, $\langle \alpha \| \hat{d} \| \beta \rangle$ is the reduced dipole operator between the orbitals α and β , and $\langle \dots \rangle_\nu$ is the mean occupation number factor. Since Ψ_ν have large numbers of principal components N , their radiative widths display small $1/\sqrt{N}$ fluctuations. This can also be seen if one recalls that a chaotic multiply-excited state is coupled by photoemission to many lower-lying states, and the total radiative width is the sum of a large number of (strongly fluctuating) partial widths. A similar effect is known in compound nucleus resonances in low-energy neutron scattering [20].

It is important to compare the radiative and autoionisation widths of chaotic multiply-excited states. Equation (12) shows that $\Gamma^{(r)}$ is comparable to the single-particle radiative widths. On the other hand, the autoionisation width $\Gamma^{(r)}$, Eq. (8), is suppressed by a factor $|C_k^{(\nu)}|^2 \sim N^{-1}$ relative to that of a typical dielectronic resonance. A comparison of Eqs.

(6) and (9) also shows that $\Gamma^{(a)}$ is suppressed as D/Γ_{spr} . Therefore, in systems with dense spectra of chaotic multiply-excited states the autoionisation widths are small. Physically this happens because the coupling strength of a two-electron doorway state is shared between many complex eigenstates. As a result, the radiative width may dominate in the total width of the resonances, $\Gamma^{(r)} \gg \Gamma^{(a)}$, making their fluorescence yield close to unity. Our numerical results for the recombination of Au^{25+} presented below, confirm this scenario.

The resonant recombination cross section should be compared to the direct radiative recombination cross section

$$\sigma_d = \frac{32\pi}{3\sqrt{3}c^3} \frac{Z_i^2}{k^2} \ln\left(\frac{Z_i}{n_0 k}\right), \quad (13)$$

obtained from the Kramers formula by summing over the principal quantum number of the final state [19]. Here Z_i is the ionic charge ($Z_i = 25$ for Au^{25+}), and n_0 is the principal quantum number of the lowest unoccupied ionic orbital. Note that the direct and resonant recombination cross sections of Eqs. (13) and (5) have similar energy dependences. Therefore, for the purpose of comparing with experiment we can evaluate the cross sections at one low energy, say $\varepsilon = 0.5$ eV. This energy is much greater than the thermal energy spread of the electron beam [2] and the cross sections can be compared directly to the experiment [1].

Using Eqs. (10) and (11) and summing over the orbitals in Fig. 1 and electron partial waves up to $h_{11/2}$, we obtain the capture cross section $\sigma_c = 23 \times 10^{-16}$ cm² at $\varepsilon = 0.5$ eV. A comparison with Eq. (6) shows that the sum which contains the autoionisation width, is

$$\sum_{J\pi} \frac{(2J+1)\Gamma^{(a)}}{(2J_i+1)D} = 0.305. \quad (14)$$

Combining this with $D = 3 \times 10^{-5}$ a.u. and taking into account that about ten different J and two parities contribute to the sum, we obtain $\Gamma^{(a)} \sim 5 \times 10^{-7}$ a.u. On the other hand, a numerical calculation of Eq. (12) gives $\Gamma^{(r)} = 3 \times 10^{-5}$ a.u. Therefore, $\Gamma^{(r)} \gg \Gamma^{(a)}$ and $\omega_f \approx 1$. Hence, the resonant recombination cross section is basically equal to the capture cross section: $\sigma_r \approx 23 \times 10^{-16}$ cm². This value is in good agreement with the experimental $\sigma^{(\text{exp})} = 27 \times 10^{-16}$ cm² [1], and exceeds the direct recombination cross section (13), $\sigma_d = 0.12 \times 10^{-16}$ cm², by a factor of 200.

In summary, we have shown that a dense spectrum of chaotic multiply-excited states can play a major role in the dynamics of electron recombination with many-electron multicharged ions, and possibly other processes, e.g. charge transfer in collisions of multiply-charged ions with neutral atoms. Based on the chaotic nature of these states, we have developed a statistical theory which enables one to calculate energy-averaged cross sections for processes which go via such resonances. Applied to the recombination of Au^{25+} , the theory shows that the contribution of resonances exceeds that of direct radiative recombination 200 times, which explains the recent experimental findings [1].

We thank Prof. A. Müller for providing experimental data in numerical form.

REFERENCES

- [†] Present address: East Antrim Institute of Further and Higher Education, Newtownabbey BT37 9RS, Northern Ireland.
- [1] A. Hoffknecht *et al.*, J. Phys. B **31**, 2415 (1998).
 - [2] The experimental energy resolution in Ref. [1] was limited by the transversal temperature of the electron beam $kT_{\perp} = 0.1$ eV.
 - [3] Below 1 meV the measured rate showed an additional enhancement. This enhancement, which depends on the electron beam temperatures T_{\parallel} and T_{\perp} and the magnetic field, is the subject of ongoing research, see, e.g., G. Gwinner *et al.*, Phys. Rev. Lett. **84** 4822 (2000). It has been observed even for bare ions, H. Gao *et al.*, J. Phys. B **30**, L499 (1997) and O. Uwira *et al.*, Hyperfine Interact. **108**, 167 (1997), and we do not consider it here.
 - [4] H. S. W. Massey and D. R. Bates, Rep. Prog. Phys. **9**, 62 (1943).
 - [5] A. Burgess, Astrophys. J **139**, 776 (1964).
 - [6] *Recombination of Atomic Ions*, NATO ASI series, Series B: Physics: vol. 296, Eds. W.G. Graham, W. Fritsch, Y Hahn, and J. A. Tanis (Plenum Press, New York, 1992).
 - [7] L. H. Andersen, P. Hvelplund, H. Knudsen, and P. Kvistgaard, Phys. Rev. Lett. **62**, 2656 (1989).
 - [8] G. Kilgus *et al.*, Phys. Rev. Lett. **64**, 737 (1990).
 - [9] S. Schennach *et al.*, Z. Phys. D **30**, 291 (1994).
 - [10] H. Gao *et al.*, Phys. Rev. Lett. **75**, 4381 (1995).
 - [11] R. Shuch *et al.*, Hyperfine Interact. **99**, 317 (1996).
 - [12] O. Uwira *et al.*, Hyperfine Interact. **99**, 295 (1996).
 - [13] O. Uwira *et al.*, Hyperfine Interact. **108**, 149 (1997).
 - [14] W. Zong *et al.*, Phys. Rev. A **56**, 386 (1997).
 - [15] S. Mannervik *et al.*, Phys. Rev. Lett. **81**, 313 (1998).
 - [16] D. R. DeWitt *et al.*, Phys. Rev. A **50**, 1257 (1994); D. R. DeWitt *et al.*, J. Phys. B **28**, L147 (1995).
 - [17] D. R. DeWitt *et al.*, Phys. Rev. A **53**, 2327 (1996).
 - [18] D. M. Mitnik *et al.*, Phys. Rev. A **57**, 4365 (1998).
 - [19] G. F. Gribakin, A. A. Gribakina, and V. V. Flambaum, Aust. J. Phys. **52**, 443 (1999); see also physics/9811010.
 - [20] A. Bohr and B. Mottelson, *Nuclear structure*, Vol. 1 (Benjamin, New York, 1969).
 - [21] This fit is valid for $E > 1$ a.u. In the Fermi-gas model a is related to the single-particle level density at the Fermi level $g(\varepsilon_F) = 3a^2/2\pi^2$. The fitted value $a = 3.35$ gives $g(\varepsilon_F) = 1.7$ a.u., in agreement with the orbital spectrum in Fig. 1.
 - [22] J. N. Ginocchio, Phys. Rev. Lett. **31**, 1260 (1973); J. Bauche and C. Bauche-Arnoult, J. Phys. B **20**, 1659 (1987).
 - [23] The level density for each configuration can be evaluated more accurately by taking its higher moments into account, see e.g. R. Karazija, *Sums of Atomic Quantities and Mean Characteristics of Spectra* (Mokslas, Vilnius, 1991), or J. Bauche, C. Bauche-Arnoult, and M. Klapisch, Adv. At. Mol. Phys. **23**, 131 (1988).
 - [24] V. Zelevinsky, B. A. Brown, M. Frazier, and M. Horoi, Phys. Rep. **276**, 85 (1996).
 - [25] V. V. Flambaum, A. A. Gribakina, G. F. Gribakin, and M. G. Kozlov, Phys. Rev. A **50**, 267 (1994); V. V. Flambaum, A. A. Gribakina, and G. F. Gribakin, Phys. Rev. A **54**, 2066 (1996); **58**, 230 (1998).

- [26] L. D. Landau and E. M. Lifshitz, *Quantum Mechanics*, 3rd ed. (Pergamon, Oxford, 1977).
- [27] Here we assume that the electron energy is below the target excitation threshold.
- [28] A detailed derivation will be published elsewhere.
- [29] V. V. Flambaum and O. K. Vorov, Phys. Rev. Lett. **70**, 4051 (1993).

FIGURES

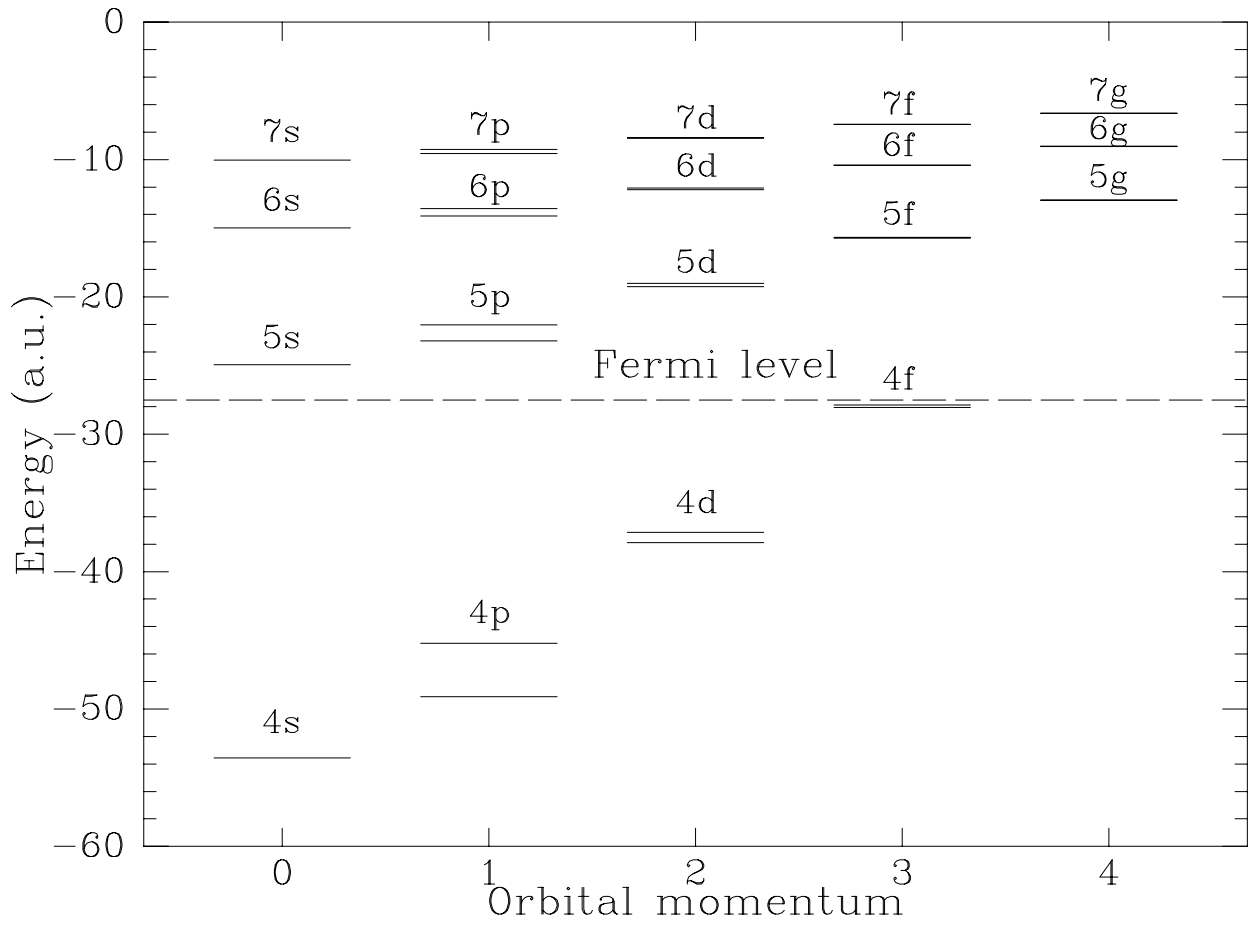


FIG. 1. Energies of the occupied and vacant single-particle orbitals of Au²⁴⁺ obtained in the Dirac-Fock calculation.